PAPER 35 (SESSION III)

The stress corrosion cracking of a non-age-hardenable aluminium alloy

R. G. WEBER* and A. J. McEVILY, Jr.†
* Graduate Student, Department of Metallurgy, University of Connecticut, Storrs, Connecticut, U.S.A.
† Professor, Department of Metallurgy and Member, Institute of Materials Science, University of Connecticut, Storrs, Connecticut, U.S.A.

Summary
The susceptibility of stress corrosion of a non-age-hardenable Al-2·5Mg-0·25Cr alloy in aqueous 3-1/2% NaCl was investigated to determine if failure of an aluminium alloy could occur in the absence of a grain boundary precipitate. Notched specimens were used, and severe corrosive attack eventually leading to failure occurred at the plastic zone at the notch root when the specimens were immersed in salt solutions made from tap water. When distilled water was used as the solvent, this severe attack did not occur. The electrochemistry of the system is discussed, and the fracture process compared with the stress corrosion behavior of age-hardened Al-5·5Zn-2·5Mg and cold-worked α-brass. Crack-tip displacement is found to be a mechanical factor of primary importance in stress corrosion

Introduction

Consideration of the stress-corrosion cracking of aluminium alloys usually centers on the influence of grain boundary precipitates and the adjacent precipitate-free regions. Relatively little attention has been given to environmentally-induced fracture processes in aluminium alloys free of such features, and with justification, since such alloys have generally proven to be satisfactory in environments which would have been disastrous for alloys containing grain boundary precipitates. However, in view of the emphasis placed upon the role of plastic deformation in certain mechanisms of stress-corrosion cracking, such as two-stage film rupture [1], it was of interest to determine whether or not failure could be induced in a homogeneous aluminium alloy under an appropriate combination of stress and environment. In selecting an alloy for such an investigation, a factor of importance is the amount of elastic strain energy available for crack propagation. Pure aluminium and solid solution alloys are so soft that it did not seem likely that a stress level could be achieved which would be high enough for cracking to occur in a reasonably short time period. However, through a combination of solid solutions strengthening and cold-working, it is possible to increase the applied stress level, and hence, the force available for crack extension, dW_e/da, where W_e is the elastic strain energy and A is the cracked area. The Al-2·5Mg alloy strengthened by cold rolling is of this type.

Materials and tests

Material

The aluminium alloy used was commercial 5052-H34 sheet, 0·020 in thick. The designation H34 indicates that the alloy was cold rolled 40% and stabilized at 150°C for 4 hours. A few check tests were also made with 0·050 in sheet. The alloying addition is nominally 2·5 w/o Mg and 0·25 w/o Cr. According to Beck and Sperry [2], up to 2 w/o Mg is soluble in aluminium, but precipitation is not appreciable until the magnesium content exceeds 3·5 w/o. Electron microscopy showed the grain boundaries of the alloy to be free of precipitation, Fig. 1. The grain size is about 50 microns, but boundaries are difficult to observe by light microscopy because of prior cold work.

The yield strength of the H34 alloy is 30,000 psi, and the tensile strength 39,000 psi.

Specimens

Single-edge-V-notched specimens ¾ inch in width were used. The notch root radius was 0·008-in, the total flank angle was 45°, and the depth ¼ in. The computed value of the elastic stress concentration factor was 5·5. The specimen surfaces were lightly polished using 0·3μ alumina polishing compound on a virgin-wool felt cloth.

Tests

Two types of loading methods were used. Some of the specimens were dead-weight loaded in a lever type creep machine, and beam deflection recorded as a function of time. Alternatively specimens were loaded to the required stress level in a Instron machine, the position of the loading head fixed, and load relaxation monitored as a function of time Specimens were mounted in a plexiglass container of 1600 cc capacity with a flexible rubber bottom slitted to allow the specimen to reach the lower grip assembly. To minimize extraneous attack the machined edges and regions remote from the notches were coated with vaseline, but even this step did not entirely eliminate water-line pitting.

The test solution was 3½% NaCl in water. In some tests distilled water (not deionized) was used, whereas in others tap water was used. Different results were obtained depending upon which type of water was used. An analysis of the tap water is given in Table 1. The solution was saturated with oxygen by using an air pump which also served to agitate the solution continuously. In order to obtain failures in less than 50 days, specimens were generally loaded in solution to 90% of the load required for failure in air.

Experiments indicated that the corrosion processes were accelerated when a constant supply of fresh solution was provided during the test.

In early tests at a flow-through rate of less than 10cc per min, corrosion products built upon the specimen surface retarding further corrosion. In such cases the reaction could be accelerated by removing the specimen, repolishing, and reloading. This procedure was unnecessary for flow rates of $\geq$ 10cc per min.

Test results

General

Several results are summarized in Table 2. These show that the combined influence of stress and a specific aqueous environment can result in premature failure of the 5052-H34 alloy. It is surprising to find that tap water is much more effective than distilled water in bringing about failure, but both Edeleanu and Evans [3] and Farmery and Evans [4] in test of other aluminium alloys have also reported this effect. Specimens stressed to the 90% load level and exposed to distilled water containing 3½% NaCl did not fail in >21 days. In fact, the load carrying capacity of specimens tested in this solution appeared to be increased slightly as compared to the failure level in air alone. This effect was also noted with notched 2-in wide specimens (stress concentration factor 8·3).

To show that both stress and environment must simultaneously be present to bring about failure, unstressed specimens were immersed in 3½% NaCl-tap water solution for three weeks and then loaded to failure in air. These specimens exhibited no loss in strength. Other specimens were loaded in air to the same 90% stress level as in the environmental tests. These specimens underwent a small amount of transient creep, but showed no sign of failure after three weeks. That both stress and environment must be present simultaneously for failure to occur is consistent with a general definition of the stress-corrosion process.

While the specimens were under load in the 3½% NaCl-tap water solution, it was observed that bubbles (thought to be hydrogen) were formed at the notch during active corrosion. Such an effect has been noted in earlier studies [5]. To a lesser extent bubble formation also occurred in the 3½% NaCl-distilled water solution. The site for bubble formation and active corrosion shifted about in time within the plastic zone, indicating a corresponding shift in the location of the local anode-cathode area. Accompanying this corrosive attack, especially at low flow-through rates, a flocculent precipitate formed in the vicinity of the notch as well as at pits on the surface. This precipitate is thought to be $Al(OH)_3$ [3].

The failure process is shown in Fig. 2. Corrosive attack initially followed the plastic zones at the notch root, but eventually the entire region within these zones was corroded. The corroded zone increased in size until, with about 10% of the total life remaining, a fine crack appeared which then grew to failure. The mechanical aspect of the failure process appeared to

dominate the final stage, as similar fine cracks were observed in tensile tests of notched specimens in air.

A plot of specimen elongation as a function of time for a constant load test in 3½% NaCl-tap water and in air is shown in Fig. 3.

Pitting experiments

Because the failure process was found to be sensitive to minor differences in the test environment, additional studies were undertaken to clarify the factors involved. Strips of alloy were immersed in an inclined position in covered beakers containing unstirred:

(a) distilled water
(b) 3½% NaCl in distilled water
(c) tap water
(d) 3½% NaCl in tap water

Following removal after one week surfaces differed significantly in appearance, Fig. 4. Table 3 summarizes the observations of surface appearance and pitting characteristics. The pitting noted in still distilled water plus 3½% NaCl was not observed in the stress-corrosion tests where the solution was under constant agitation. The elliptical regions surrounding the pits formed in tap water indicated that a gravitational effect was present. Similar regions around pits formed on the specimen's underside but were much smaller than on the upper surface. The corrosion protection adjacent to the pits may be due to the deposition of a flocculent product around each of these pits. This appeared to be the same flocculent product as that which formed at the plastic zone in the stress-corrosion test. Fig. 5 shows the appearance of a specimen after stressing for two weeks in tap water containing 3½% NaCl. Note the similarity between the protected regions adjacent to the corroded zone at the notch root and regions adjacent to the pits. Corrosive attack is also evident along slipbands away from the notch.

Discussion

Electrochemical effects

Fig. 6 indicates some of the chemical reactions involved in the pitting of aluminium [3]. Although not indicated, a counter-flux of Cl^{-1} ions and Al^{+++} ions through a surface film may take place [6]. When hydrogen is evolved the pH within the pit (or crack) should decrease. This reaction will be arrested as the $Al(OH)_3$ precipitate covers the pit walls and thereby screens the H^+ ions from the cathodic area.

In the present experiments it appears that both cathodic reactions were operative. Hydrogen was observed to emanate from pits, and to an even

greater extent from the plastic zone under stress corrosion conditions. Also $Al(OH)_3$ was formed in both types of experiment, and a pH rise from 6·5 to 7·5 was observed. Evans [7] suggested that hydrogen evolution is enhanced by plastic deformation. Although the alloy in the H34 condition contains many dislocations, the observed preferential attack at slipbands demonstrates the importance of active plastic deformation in the corrosion process.

Farmery and Evans [4] indicated that the HCO_3^- ion in tap water was a significant constituent. Our tests showed that by immersing a specimen in distilled water containing CaO, $NaHCO_3$, and NaCl the same general pitting behavior occurred as in tap water. Farmery and Evans surmised that the bicarbonate ion removed cathodically formed alkali that would otherwise interfere with the build-up of acidity in the pits. On the other hand, Pryor [6] has suggested that the HCO_3^- ion reacts with the H^+ ion in the pits or crack to buffer the local solution and prevent it from becoming too acidic. Too low a pH would lead to general acid attack of the pit walls and prevent the formation of deep pits by an electrochemical mechanism.

Cracking mechanisms

The present results show that 5052-H34 is susceptible to stress corrosion under certain conditions of stress and environment, and that the attack at the plastic zone has much in common with the pitting process. However, active plastic deformation serves to localize corrosive attack, whereas inhomogeneities are required for pitting. Since 5052-H34 lacks an active path for corrosion and a relatively large radius for the notch was used, attack occurred over a large area. Only in the terminal stage did a sharp crack develop, suggesting that the final crack advance was then more under mechanical than electrochemical control.

Since the site of corrosive activity shifted from point to point within the plastic zone as well as along the surface of the advancing crack tip, the crack advance was locally intermittent in nature. Time-dependent plastic deformation served to break or thin the surface oxide film, thereby allowing dissolution of the base metal to take place at such deformed sites more readily than elsewhere. This localized attack at a particular site terminated as corrosion products formed, and as plastic deformation in breaking down surface films led to the creation of more active sites elsewhere. Failure resulted then from a summation of many individual film-rupture and dissolution events.

Comparison of this type of cracking with two other instances of stress-corrosion cracking indicates the variations in cracking mode which can arise.

In the case of cold-worked α-brass [8] each increment of crack advance was considered to consist of two components. One component was the thickness of a substitutional tarnish film, f_f, at the crack tip, Fig. 7 (a). The

other was the distance advanced by plastic deformation, m, before the crack was arrested because of blunting in the ductile substrate. For this model the following expression was developed for the rate of crack growth, $\Delta c/\Delta t$,

$$\frac{\Delta c}{\Delta t} = A(\sigma\sqrt{c})^n, \text{ where } A \text{ is a constant.}$$

Analysis of experimental results indicated that an appropriate value for the exponent n is 2. This result led to the conclusion that the rate of crack growth is dependent upon the crack tip displacement, since this quantity also is proportional to the square of the stress intensity factor.

Next consider the stress-corrosion cracking behavior in a NaCl solution of an Al-5·5Zn-2·5Mg alloy in the quenched and aged condition where cracks followed an intergranular path [9]. There was no strong evidence of a two-stage mechanism, although slip markings were observed at micron intervals. The presence of $MgZn_2$ particles in the grain boundary is a major factor in determining the active path for cracking, and it appears that the corrosion and tearing mechanism of Dix *et al.* [10], is operative in this case. The presence of zones denuded of precipitate and depleted of solute adjacent to the grain boundaries also serves to localize the cracking path by concentrating plastic deformation within these zones. We can derive a relationship between the rate of crack growth and stress intensity factor as follows:

Fig. 7 (b) is a schematic of the grain boundary structure through which the crack advances. The thin, disc-like particles of Mg-Zn_2 will dissolve preferentially, as they are anodic to the adjacent solute free zones. The tensile stress will contribute to the advance of the crack by fine scale tearing of regions adjacent to dissolved regions. As indicated in Fig. 7 (b) there is a characteristic repeat distance, Δl, which is related to the size of the grain boundary precipitate particles. The time interval to advance the crack front by Δl is taken to be inversely proportional to the corrosion rate and to a power n of the stress intensity factor. The rate of crack advance is then

$$\frac{\Delta l}{\Delta t} = B(\sigma\sqrt{l})^n, \text{ where } B \text{ is a constant.}$$

Analysis of experimental results indicated that the value of n in this case was also 2 so that, as for α-brass, the rate of crack growth is dependent upon the crack tip displacement.

In the case of the 5052-H34 alloy the failure mechanism incorporates features of both of these mechanisms, namely intermittent film rupture as in the case of brass, and dissolution as in the case of the Al-Zn-Mg alloy. A main difference is the absence of an active path for cracking. However,

even in this case the rate of cracking is likely to be dependent upon the crack tip displacement, since the size of the plastic zone at the crack tip is directly related to tip displacement, and it is this zone which is preferentially attacked. In each of the cases cited then, crack tip displacement emerges as a factor of importance in governing the rate of stress corrosion.

Conclusions

1. Stress-corrosion failure of aluminium alloy 5052-H34 can be induced in tap water containing 3½% NaCl, but because of the absence of an active path, the cracking process differs from that in more susceptible alloys.
2. The cracking process of this alloy is sensitive to minor constituents of the environment, especially bicarbonate ion concentration.
3. Crack tip displacement is believed to be a factor of general importance in determing the rate of stress-corrosion cracking.

Acknowledgements

The authors wish to acknowledge the helpful discussions with Drs M. J. Pryor, J. Ford, A. R. C. Westwood, and A. P. Bond, and we thank Mr J. J. Harwood of the Ford Motor Company for the loan of test apparatus. This work was supported in part by a grant of the University of Connecticut Research Foundation, and in part, by U.S. Air Force Contract F44620 69C011.

References

1. FORTY, A. J. & HUMBLE, P. *Phil. Mag.*, vol. 8, p. 247, 1963.
2. BECK, A. F. & SPERRY, P. R. Conference on Fundamental Aspects of Stress Corrosion Cracking, Ohio State University, Columbus, Ohio, Sept. 1967.
3. EDELEANU, C. & EVANS, U. R. *Trans. Faraday Soc.*, vol. 47, p. 1121, 1951.
4. FARMERY, H. K. & EVANS, U. R. *J. Inst. of Metals*, vol. 84, p. 413, 1955-56.
5. GILBERT, P. T. & HADDEN, S. E. *J. Inst. of Metals*, vol. 77, p. 237, 1950.
6. PRYOR, M. J. private communication, 1968.
7. EVANS, U. R. *J. Inst. of Metals*, vol. 80, p. 708, 1951-52.
8. McEVILY, A. J. & BOND, A. P. *J. Electrochm. Soc.* vol. 112, p. 131, 1965.
9. McEVILY, A. J., CLARK, J. B. & BOND, A. P. *Trans. of the ASM*, vol. 60, p. 661, 1967.
10. DIX, E. H. *Inst. of Metals Div., Am. Inst. Mining Eng.*, vol. 137, p. 11, 1940.

Table 1
Analysis of local tap water

Physical:	
pH	6·3-6·6
Chemical:	ppm
Nitrite	0·0
Nitrate	12
Chloride	12
Bicarbonate	12
Carbonate	0·0
Iron	0·3
Total hardness	24

Table 2
Test results

Specimen number	*Specimen orientation*	*Time to failure (days)*	*% of failure load in air*	*Solvent with 3½% NaCl*	*Apparatus type*
1	Longitudinal	41	93%	Distilled[a] and tap water	Fixed displacement
2	Longitudinal	36	90%	Distilled[a] and tap water	Fixed displacement
3	Longitudinal	20	82%[c]	Tap water	Fixed displacement
4	Transverse	22	90%	Tap water	Fixed displacement
5	Transverse	18	90%	Tap water	Fixed load
6	Transverse	17·5	90%	Tap water	Fixed load
7	Transverse	>21[d]	90%	Distilled water	Fixed load
8	Transverse	>21[d]	90%	Distilled water	Fixed load

a. Distilled water was used initially but solution replenishment was made with tap water.
b. This specimen was 0·050 in thick. There was no qualitative difference in behavior between this specimen and the 0·020 in thick specimens.
c. Initially loaded to 92% of failure stress in air for seven days without sign of cracking. Specimen then repolished and loaded to 82% load level.
d. No evidence of corrosive activity in this time period.

Table 3
Surface observations

Solution	*Macroscopic (1×)*[a]
A. Distilled water	1. Luster of 'as received' material 2. Random pitting
B. Distilled water plus 3½% NaCl	1. Greyish film 2. Uniform pitting, 15 pits/cm^2
C. Tap water	1. Brownish film 2. Severe random pitting
D. Tap water plus 3½% NaCl	1. Characteristics of both B and C

a. On the microscopic (200×) level surfaces were uniformly pitted with approximately 400 pits/cm^2.

Fig. 1. Grain boundary region of 5052-H34. (60,000 ×)

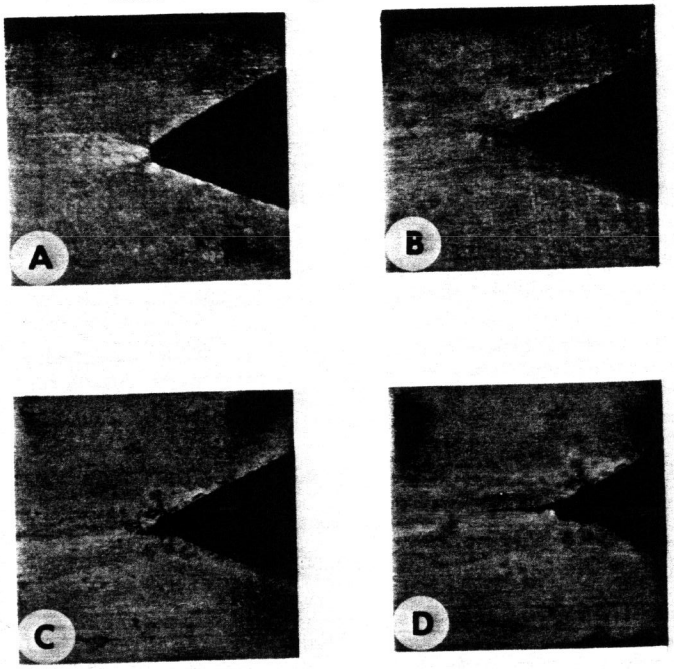

Fig. 2. Progress of failure process at root of notch. (12×)

A. 1st day
B. 7th day
C. 21st day
D. 22nd day

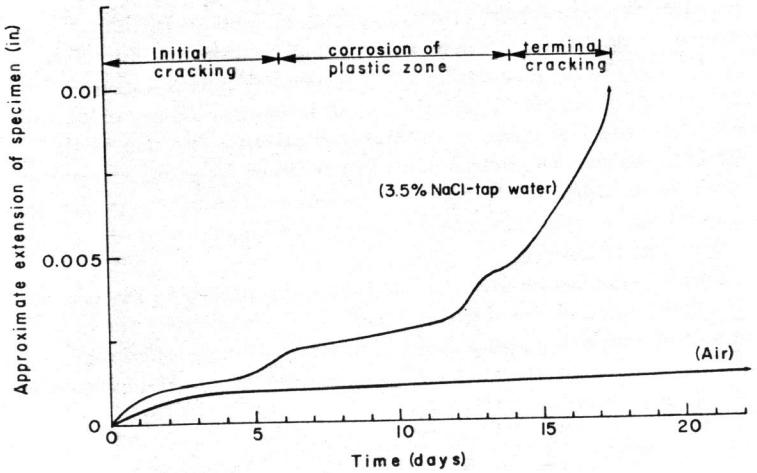

Fig. 3. Approximate specimen extension as a function of time.

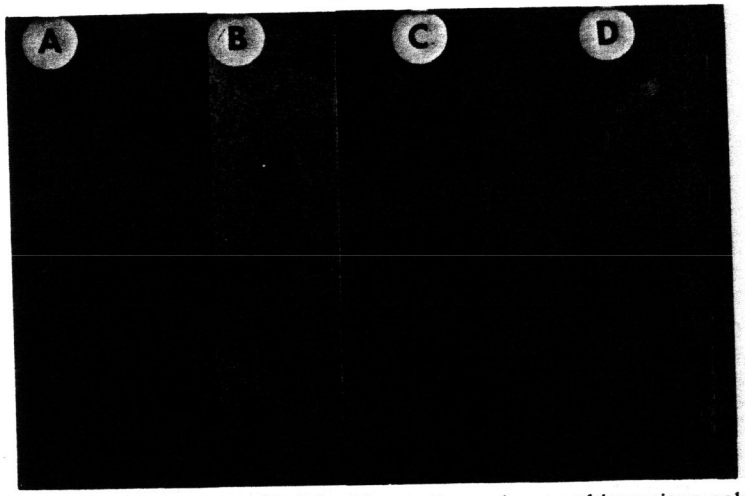

Fig. 4. Surface appearance of ¾ inch wide specimens immersed in various solutions:
A. Distilled Water
B. Distilled Water plus 3·5% NaCl.
C. Tap Water
D. Tap Water plus 3·5% NaCl.

Fig. 5. Pits, protected areas, and slip bands developed on specimen stressed in 3·5% NaCl—tap water for two weeks. (9·6 ×)

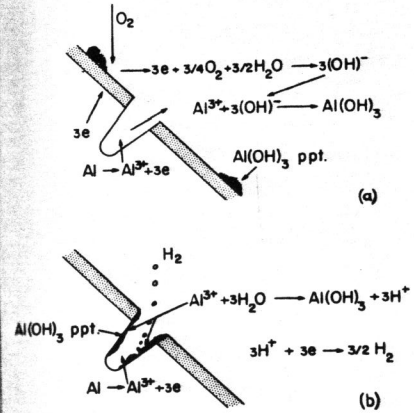

Fig. 6. Reactions associated with the pitting process.

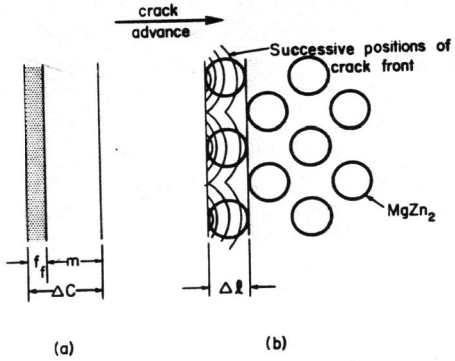

Fig. 7. Schematic of stress corrosion process
(a) Film rupture mechanism
(b) Particle dissolution with tearing mechanism